Avalanche Breakdown Calculations for a

Planar p-n Junction*

Abstract: A mathematical analysis is presented on the avalanche breakdown voltage of a planar p-n junction. This analysis takes into consideration junction curvature, as encountered near a diffusion mask edge. Three different impurity atom profiles are considered: abrupt, linearly graded, and diffused. For an asymmetrical abrupt structure, it is shown that regions of junction curvature exhibit either an increase or a decrease in avalanche breakdown voltage. It is also shown that similar regions in a linearly graded junction exhibit a combination of these abrupt junction mechanisms; thereby, their breakdown voltage is little influenced by junction curvature. In addition, the diffused planar junction can be designed to exhibit nearly the same breakdown voltage as a corresponding mesa structure, or, instead, it can be designed to exhibit a substantially lower avalanche breakdown voltage.

Introduction

Planar transistor technology has become universally accepted in the fabrication of high frequency devices. However, it has been found that junctions produced by planar techniques usually exhibit a lower avalanche breakdown voltage than corresponding mesa junctions. The purpose of this paper is to present a mathematical analysis of junction curvature, one of the mechanisms contributing to the reduced avalanche breakdown voltage encountered in planar structures. This subject has been discussed by many authors, ¹⁻³ yet insufficient information is available for practical engineering purposes.

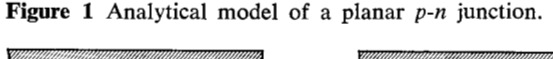
Avalanche breakdown voltage calculations for a mesa p-n junction are available in the literature, $^{4-6}$ although this work is only partially applicable to structures of planar geometry. In fact, it will be shown that the avalanche breakdown voltage of a diffused mesa junction represents an upper bound for the breakdown encountered in a diffused planar junction. This situation arises from modifications of the space-charge electric field near a diffusion mask edge. In this region, the breakdown voltage of a planar junction depends not only on the physical constants of the semiconductor, but also upon its radius of curvature.

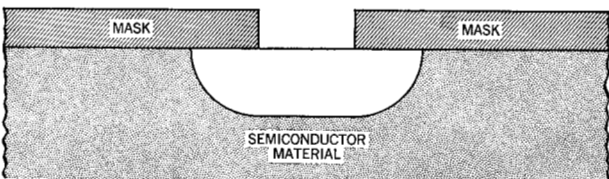
It is often shown^{5,7} that a diffused *p-n* junction can be designed to exhibit characteristics similar to a linearly graded junction or, instead, it can be designed to exhibit

characteristics similar to an asymmetrical abrupt junction. This situation is again encountered in a mathematical analysis of avalanche breakdown in diffused planar *p-n* junctions. For this reason, the present analytical investigation has been divided into separate discussions on the avalanche breakdown characteristics of asymmetrical abrupt and linearly graded *p-n* junctions. Thereafter, the characteristics encountered in these two types of structures are shown to exist simultaneously within a diffused planar device. This combination of avalanche breakdown characteristics is used to explain why some diffused planar junctions exhibit a substantially lower breakdown voltage than corresponding mesa structures, while others exhibit essentially the same avalanche breakdown voltage as a corresponding mesa structure.

The impurity atom distribution in a diffused planar junction

Figure 1 illustrates the mathematical model used in this





*The analysis presented in this paper was supported in part by the Air Force Cambridge Research Laboratories, Office of Aerospace Research, under Contract AF 19(628)-5072, Project 4608.

investigation. Assuming a diffusion mask upon the semiconductor surface, an opening is first made in this mask, and thereafter impurity atoms are diffused into the semiconductor material. Throughout this analysis diffusion is assumed to take place from a constant-density impurity atom source residing upon the semiconductor surface. Figure 1 is a two-dimensional illustration of the semiconductor material after completing this junction fabrication process.

In a previous investigation,⁸ the impurity atom distribution in a diffused planar p-n junction was shown to be characterized by an infinite series,

$$C(r, \theta, t) = C_0 \left\{ 1 - \frac{2}{\pi} \sum_{n=0}^{\infty} \sin(s_n \theta) \right.$$

$$\times \frac{\left[(r/2) Dt \right]^{s_n} \Gamma(s_n/2)}{2\Gamma(s_n + 1)} {}_{1}F_{1} \left[\frac{s_n}{2} ; s_n + 1; \frac{r^2}{4 Dt} \right] \right\}, \quad (1)$$

where the hypergeometric function ${}_{1}F_{1}[\alpha; \beta; \gamma]$ is given by

$$_{1}F_{1}[\alpha;\beta;\gamma] = \sum_{k=0}^{\infty} \frac{\alpha_{k}}{k!\beta_{k}} \gamma^{k},$$
 (2)

and

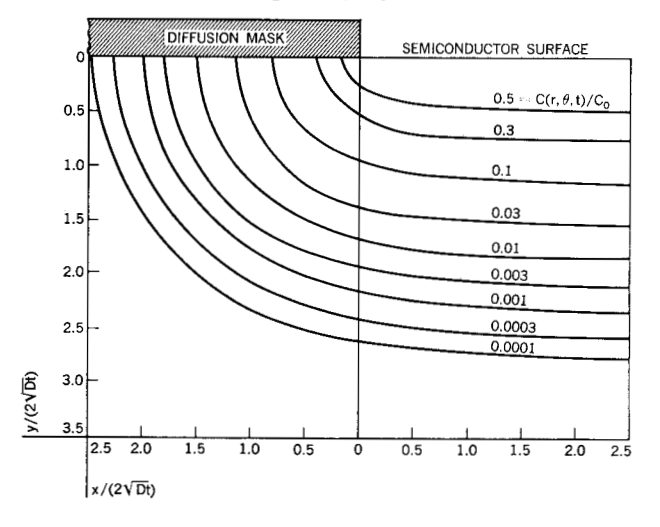
(a)
$$h_k = h(h+1)(h+2)$$

 $\times (h+3) \cdots (h+k-1), \quad h_0 = 1,$
(b) $s_n = (n+\frac{1}{2}).$ (3)

Figure 2 illustrates theoretical p-n junction profiles, from Eq. (1), in the immediate vicinity of a diffusion mask edge.

In Fig. 2, the junction curvature cannot be rigorously described by an elementary mathematical equation. The junction penetration depth under a diffusion mask (along the semiconductor-diffusion mask boundary) is less than

Figure 2 Calculated contours of constant impurity atom density at the edges of a planar p-n junction.



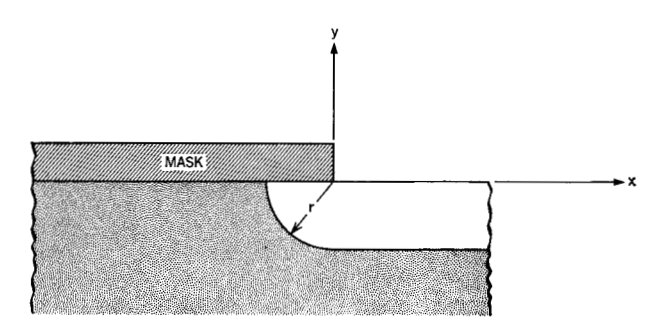


Figure 3 Circular cylinder approximation for the edge of a planar p-n junction.

the junction penetration depth perpendicular to the semiconductor surface (at the center of the diffusion mask opening). This difference of junction penetration becomes particularly evident when a small difference exists between the impurity atom density within the bulk material, C_b , and the concentration of impurity atoms upon the exposed surface, C_0 .

A detailed calculation of the impurity atom distribution in Fig. 2 has been discussed in a previous publication. It was shown that Eq. (1) describes a complementary error function type of distribution in a direction perpendicular to the semiconductor surface (at the center of the diffusion mask opening). Furthermore, the impurity atom distribution along the semiconductor-diffusion mask boundary can be approximated by a complementary error function from which a constant is subtracted. Although this description is admittedly an approximation, it provides a qualitative explanation for the existence of a constant impurity atom concentration gradient within a planar junction space-charge layer while, simultaneously, its metallurgical junction is not a constant distance from the exposed semiconductor surface.

The present analysis is based upon a simple approximation for the junction profile encountered in a practical planar structure. It is assumed that the edge of a two-dimensional planar junction can be approximated by a circle (Fig. 3), thereby neglecting breakdown mechanisms occurring at the diffusion mask corners. In this mathematical model, the radius of junction curvature r is set equal to the maximum junction penetration depth in a direction perpendicular to the semiconductor surface. Furthermore, in this simplified model, the impurity atom distribution in a diffused planar structure is approximated by Eq. (1) along the diffusion mask-semiconductor interface.*

^{*} A similar impurity atom distribution was used in the calculation of avalanche breakdown in diffused mesa p-n junctions (Ref. 5). It is now recognized that this previous calculation is applicable to structures containing a substantially different impurity atom distribution, provided a known impurity gradient exists at the metallurgical junction.

Carrier multiplication in an infinite cylindrical p-n junction

The depletion layer theory of a p-n junction provides a relatively uncomplicated picture of the mechanisms encountered in this device. At large values of reverse biasing voltage, the space-charge region is assumed completely depleted of mobile charge carriers (holes and electrons). This approximation implies that the electrostatic potential within a cylindrical p-n junction (of infinite length) is fully described by a one-dimensional form of Poisson's equation,

$$\frac{d^2\psi}{dr^2} + \frac{1}{r}\frac{d\psi}{dr} = \frac{q}{\kappa\epsilon_0}C(r),\tag{4}$$

where C(r) represents the distribution of ionized impurity atoms along a radius vector r.

At large values of applied biasing voltage, the electric field within this space-charge region becomes sufficient to cause impact ionization of the semiconductor lattice by mobile charge carriers. If we assume an identical ionization rate, α_i , for holes and electrons, the total carrier multiplication M within a p-n junction becomes

$$1 - \frac{1}{M} = \int_0^w \alpha_i(r) dr, \qquad (5)$$

where w is the space-charge layer width, $\alpha_i(r)$ is given by the equation*

$$\alpha_i(r) = a \exp(-b/|E(r)|), \tag{6}$$

and E(r) is the space-charge layer electric field.

The theoretical avalanche breakdown voltage is established in a similar fashion for all types of cylindrical p-n junctions (abrupt, linearly graded, and diffused). Poisson's equation (4) is numerically solved throughout the structure under consideration; thereby we obtain its spacecharge electric field distribution, E(r). This electric field distribution, in combination with Eqs. (5) and (6), provides a means for calculating carrier multiplication M within a given p-n junction, at a specified space-charge layer width w. The space-charge layer width is thereafter iterated until a value w' is attained that satisfies the equality

$$1 = \int_0^{w'} \alpha_i(r) dr.$$

At this point the calculated carrier multiplication M becomes infinite, and a condition of avalanche breakdown exists within the structure under consideration. The avalanche breakdown voltage V_b is established by calculating the total junction potential resulting from this spacecharge layer width w'.

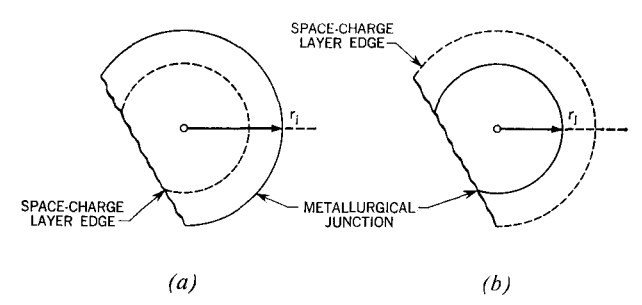


Figure 4 Cylindrical, asymmetrical, abrupt *p-n* junctions: (a) infinite electrical conductivity outside cylinder; (b) infinite electrical conductivity inside cylinder.

Asymmetrical abrupt *p-n* junction of cylindrical geometry

The avalanche breakdown characteristics of a diffused planar p-n junction can be explained by first considering the breakdown characteristics of an asymmetrical abrupt junction of cylindrical geometry (Fig. 4). For this purpose we shall consider only ideal asymmetrical abrupt structures containing an infinite electrical conductivity on one side of the metallurgical junction (r_i) and a finite electrical conductivity on the other side. This type of analytical model permits us to separate the two types of space-charge layer distortion resulting from junction curvature: One type occurs when the space-charge layer resides inside the circular cylinder bounded by the metallurgical junction (Fig. 4a), and a second type occurs when the space-charge layer resides outside the cylinder (Fig. 4b).

First, let us consider the space-charge layer characteristics of an abrupt p-n junction containing an infinite electrical conductivity outside the cylindrical region under consideration (Fig. 4a). This type of structure restricts the space-charge layer to the region inside the cylinder. It should be observed that a junction of this particular configuration (circular cylinder) exhibits what could be called a maximum avalanche breakdown voltage. At some externally applied reverse biasing voltage, the space-charge layer will penetrate to the center of this cylinder, and the entire cylinder thereby becomes a space-charge region. Because this cylindrical junction has been adopted to approximate the edge of a planar structure, junction mechanisms are of little interest when they occur at a biasing voltage above this cylinder penetration voltage. If the space-charge layer of a cylindrical junction (Fig. 4a) penetrates to the center of the cylinder, it is implied that the space-charge layer of a corresponding planar junction has penetrated to the semiconductor surface.

From a general solution of Eq. (4), the space-charge layer electric field within an abrupt cylindrical junction is given by

$$E(r) = -\frac{d\psi}{dr} = -\frac{qC_b}{2\kappa\epsilon_0} \frac{(r^2 - K)}{r}, \qquad (8)$$

^{*} The constants (a and b) in this expression have been previously discussed by the authors in Ref. 6. For purposes of this analysis, in germanium $a=1.65\times10^7$ and $b=1.422\times10^9$, while in silicon $a=1.47\times10^9$ and $b=1.875\times10^9$.

where K is an arbitrary constant. If we next assume this electric field is zero at r = 0, Eq. (8) becomes

$$E(r) = -\frac{qC_b}{2\kappa\epsilon_0}r, (9)$$

and for the total difference of potential across this p-n junction we obtain

$$V(r) = \frac{qC_b}{4\kappa\epsilon_0} r^2. \tag{10}$$

Equation (9) can now be substituted into Eq. (7), yielding an expression of the form

$$1 = a \int_0^{r_i} \exp \left\{-b / \frac{qC_b r_i}{2\kappa \epsilon_0} \left[1 - (r/r_i)\right]\right\} dr. \tag{11}$$

From Eq. (11), we can establish the space-charge layer width (and hence the junction radius of curvature since $w = r_i$) at which avalanche breakdown occurs. A Taylor series expansion is used to simplify the exponent in Eq. (11),

$$1 \cong a \int_0^{r_i} \exp\left[-\frac{2b}{C_b r_i q/\kappa \epsilon_0} \left(1 + \frac{r}{r_i} + \frac{r^2}{r_i^2}\right)\right] dr. \quad (12)$$

After solving Eq. (12) for the space-charge layer width, and thereafter determining the implied breakdown voltage V_b , we have

$$V_b \cong \frac{9b^2/(4qC_b/\kappa\epsilon_0)}{\left\{ \text{Log}_{\epsilon} \left[\frac{V^{3/2}\pi a^2}{b(C_bq/\kappa\epsilon_0)^{1/2}} \operatorname{erfc}^2 \left(\frac{\sqrt{b}}{2(qC_bV_b/\kappa\epsilon_0)^{1/4}} \right) \right] \right\}^2}.$$
(13)

From a previous investigation of avalanche breakdown.⁶ we can readily interpret the foregoing analysis. If a bulk impurity atom density of $C_b/2$ (instead of C_b) is substituted into Eq. (13), this equation becomes identical to the avalanche breakdown voltage of an abrupt mesa $(r = \infty)$ p-n junction. From a physical point of view, this situation implies that junction curvature of the type illustrated in Fig. 4a increases the avalanche breakdown voltage of an asymmetrical abrupt p-n junction. Furthermore, this increase of avalanche breakdown voltage will continue (with a decreasing radius of curvature) until the junction spacecharge layer extends throughout the entire cylindrical structure. This maximum avalanche breakdown voltage is identical to the value obtained in a mesa junction $(r = \infty)$ containing an impurity atom density of $C_b/2$, rather than C_h .

Substantially different avalanche breakdown characteristics are encountered in abrupt cylindrical junctions of the type illustrated in Fig. 4b. In this structure, a decrease of avalanche breakdown voltage is obtained by a decrease in radius of curvature. This reduction of avalanche breakdown voltage has no apparent theoretical limit. A continuous decrease in the radius of curvature results in a

continuous decrease of the breakdown voltage, until other breakdown mechanisms dominate and carrier multiplication is therefore no longer an important factor.

The foregoing avalanche breakdown characteristics imply an important physical property of cylindrical junctions. In a given p-n junction, avalanche breakdown occurs at an approximately constant magnitude of maximum space-charge layer electric field, regardless of the radius of curvature. Therefore, if a change in radius of curvature results in a change in avalanche breakdown voltage, it must be concluded that significant modifications occur in the junction space-charge layer width. For example, in the p-n junction illustrated by Fig. 4a, a decrease in radius of curvature increases the avalanche breakdown voltage; thereby, an increase is implied in its space-charge layer width. Similarly, the structure illustrated in Fig. 4b undergoes a decrease in avalanche breakdown voltage with a decrease in radius of curvature; this situation implies a decrease in space-charge layer width. These qualitative conclusions have been verified by a detailed mathematical analysis of the problem.

Figures 5 and 6 illustrate the numerically calculated avalanche breakdown voltage for asymmetrical abrupt p-n junctions (cylindrical geometry) in silicon and germanium, respectively. Each illustration contains the calculated breakdown voltage for the two structures shown in Fig. 4. The contour $r = \infty$ (in Figs. 5 and 6) presents the breakdown voltage for a junction of infinite radius of curvature (for example, an abrupt mesa junction). All breakdown voltages lying above the $r = \infty$ contour apply to asymmetrical abrupt junctions of the type shown in Fig. 4a. Breakdown voltages below the $r = \infty$ contour are applicable to asymmetrical abrupt junctions of the type shown in Fig. 4b. Further, all contours lying above $r = \infty$ have been terminated at the cylinder penetration voltage.

Linearly-graded p-n junction of cylindrical geometry

A linearly graded junction of cylindrical geometry simultaneously exhibits the avalanche breakdown characteristics outlined for both types of asymmetrical abrupt *p-n* junctions (Fig. 4). A decrease in radius of curvature modifies the avalanche breakdown space-charge width on both sides of a linearly graded junction. Inside the circular cylinder, the space-charge region undergoes a substantial increase of width at avalanche breakdown (with a reduction in radius of curvature), and this increase contributes to an increase in the breakdown voltage. Simultaneously, the space-charge region lying outside the cylinder undergoes a decrease of width (with a decrease in radius of curvature), and this modification contributes to a reduction of the avalanche breakdown voltage. This simultaneous increase of space-charge layer width on one side and decrease of

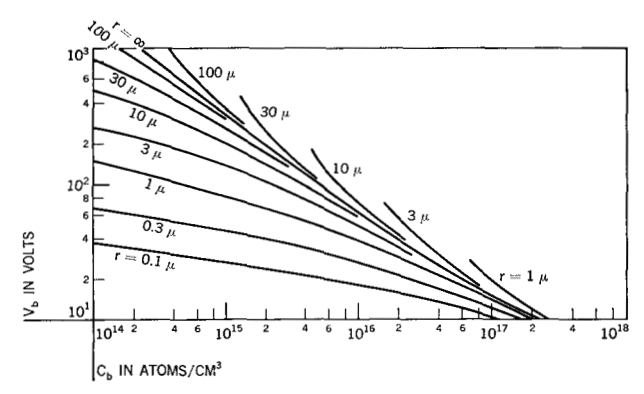
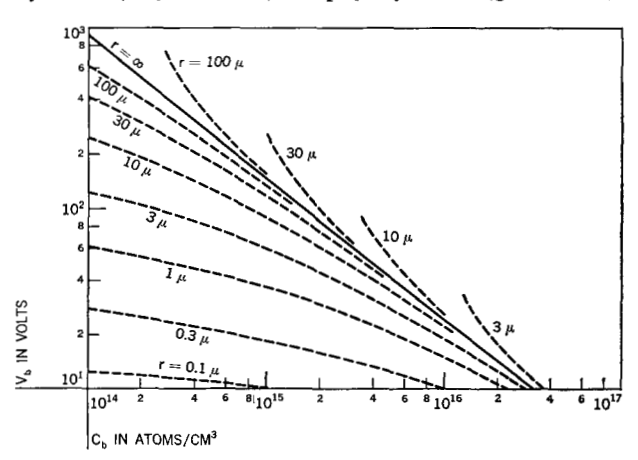


Figure 5 Calculated avalanche breakdown voltage for a cylindrical, asymmetrical, abrupt p-n junction (silicon).

Figure 6 Calculated avalanche breakdown voltage for a cylindrical, asymmetrical, abrupt p-n junction (germanium).



width on the other side reduces the influence of junction curvature upon the avalanche breakdown voltage. For a linearly graded junction of cylindrical geometry, only small variations are observed in its calculated avalanche breakdown voltage, with a change in radius of curvature.

At some specified reverse biasing voltage, the space-charge of this linearly graded junction will penetrate to the center of the cylinder; the entire cylinder thereby becomes a space-charge region. It is emphasized that this cylindrical geometry has been adopted to only approximate a linearly graded planar structure. For this reason, junction mechanisms are of little interest when they occur at biasing voltages above this condition of cylinder penetration. If the space-charge region penetrates the entire cylinder, the space-charge of a corresponding planar junction has penetrated to the semiconductor surface.

In this analysis, the simultaneous occurrence of avalanche breakdown and surface penetration represents a

limiting condition that can be mathematically established. Poisson's equation for a linearly graded cylindrical junction has the form

$$\frac{d^2\psi}{dr^2} + \frac{1}{r}\frac{d\psi}{dr} = -\frac{q\Omega_0}{\kappa\epsilon_0}(r - r_i),\tag{14}$$

where α_0 is the concentration gradient of ionized impurity atoms, and r_i locates the metallurgical p-n transition from n-type to p-type material. In addition, the parameter r_i represents the radius of curvature for this cylindrical p-n junction. After assuming the electric field E(r) is zero at r=0 (implying that the junction space-charge extends throughout the entire cylinder), we obtain from Eq. (14)

$$E(r) = \frac{q}{\kappa \epsilon_0} \alpha_0 \left(\frac{r^2}{3} - \frac{r}{2} r_i \right). \tag{15}$$

From Eq. (15), the total difference of potential across this linearly graded cylindrical junction is

$$V = -\frac{9}{48} \frac{q\Omega_0}{\kappa \epsilon_0} r_i^3. \tag{16}$$

Equation (15) can now be substituted into Eq. (7), yielding an expression of the form

$$1 = a \int_0^{3r_i/2} \exp\left\{\frac{-b}{\alpha_0 q[(r^2/3) - (rr_i/2)]/\kappa \epsilon_0}\right\} dr. \quad (17)$$

After a change of variables in Eq. (17), and a Taylor series expansion of the exponent, we obtain

$$1 \cong a \int_{-r_i}^{r_i/2} \exp\left\{\frac{-b}{q\Omega_0 r_i^2/6\kappa\epsilon_0} \left[1 + \frac{\xi}{r_i} + \frac{3\xi^2}{r_i^2}\right]\right\} d\xi. \quad (18)$$

From the solution of Eq. (18), the space-charge layer width (r_i) at avalanche breakdown is given by

$$r_i = \frac{\exp(11\eta^2/36)}{(\sqrt{\pi}a/2\eta) \left[\text{erfc} (5\eta/6) + \text{erfc} (4\eta/6) \right]},$$
 (19)

where

$$\eta^2 = \frac{18b}{a\Omega_0 r_i^2/\kappa\epsilon_0}. (20)$$

In combination, Eqs. (16) and (19) establish the junction biasing voltage at which avalanche breakdown occurs simultaneously with cylinder penetration by the p-n junction space-charge layer.

Figure 7 illustrates a numerical solution of Eqs. (4), (6), and (7) for the avalanche breakdown voltage of a linearly-graded p-n junction (cylindrical geometry) in both silicon and germanium. This calculation shows that a cylindrical junction should exhibit a slightly larger avalanche breakdown voltage than an equivalent mesa $(r = \infty)$ junction. In Fig. 7, the individual contours of constant radius of curvature r have been terminated at the simultaneous occurrence of cylinder penetration and avalanche breakdown.

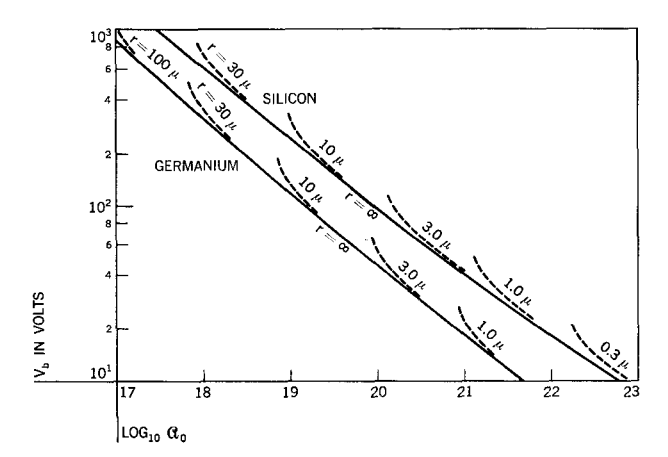
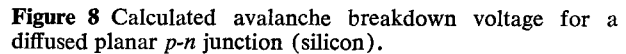
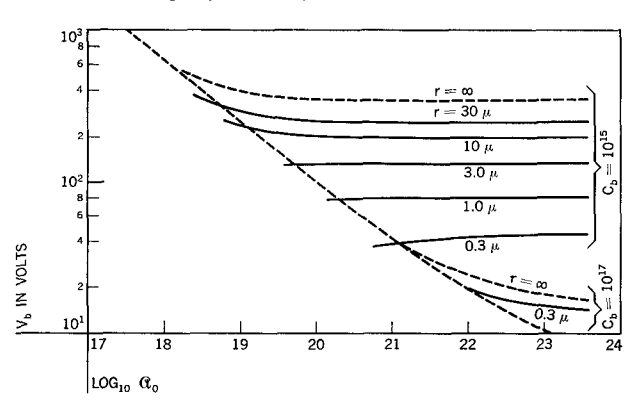


Figure 7 Calculated avalanche breakdown voltage for a cylindrical, linearly graded p-n junction.





Diffused p-n junction of cylindrical geometry

In a previous publication, 5 it was shown that the basic design of a diffused mesa p-n junction has a significant influence upon its avalanche breakdown voltage. At small values of impurity atom gradient, a diffused mesa junction exhibits the same avalanche breakdown voltage as an equivalent linearly graded structure. If, instead, a large impurity atom gradient is used in the design of this same device (maintaining constant doping levels throughout), its avalanche breakdown voltage decreases to a value comparable to that of an abrupt asymmetrical junction. For the diffused mesa junction, the theoretical avalanche breakdown can be approximated by a linearly graded model, an asymmetrical abrupt model, or by a structure lying between these two elementary models.

This situation arises again in the design of a diffused planar *p-n* junction, and it has a profound influence upon its avalanche breakdown voltage. It is a universal practice to design planar junctions from the theoretical breakdown

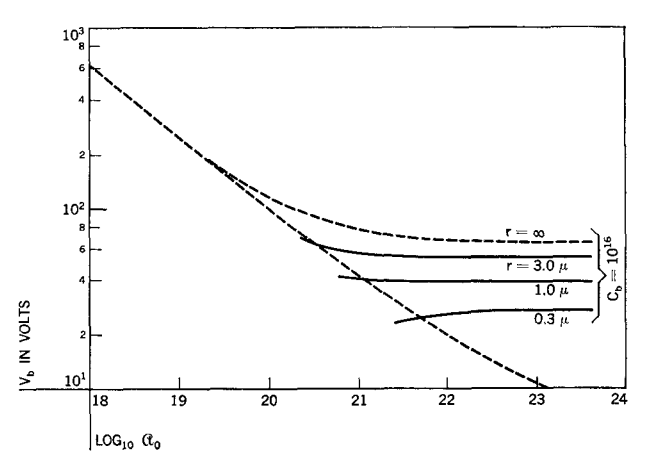


Figure 9 Calculated avalanche breakdown voltage for a diffused planar p-n junction (silicon).

characteristics of diffused mesa junctions (using, for example, Ref. 5). This practice can lead to planar junctions that exhibit the same calculated breakdown voltage as an equivalent mesa structure, or, instead, it can lead to planar junctions that exhibit a substantially lower breakdown voltage.

Consider, for example, the breakdown characteristics of a diffused planar junction intentionally designed (from the breakdown properties of a mesa junction⁵) to exhibit the avalanche breakdown voltage of an equivalent linearly-graded structure. For purposes of simplification, we assume the radius of curvature in this planar junction is not sufficient to cause space-charge penetration to the semi-conductor surface. From the breakdown properties of a cylindrical linearly graded junction (Fig. 7), regions of curvature in the planar structure exhibit a larger avalanche breakdown voltage than the region parallel to the semi-conductor surface (see Fig. 1). This situation implies that comparable junctions of mesa and planar geometry (containing a small impurity atom gradient) exhibit the same theoretical avalanche breakdown voltage.

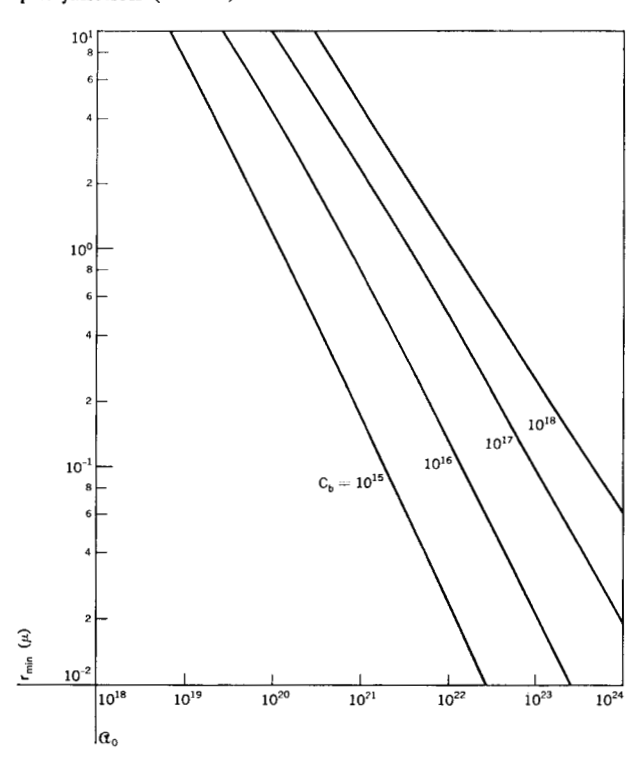
A substantially different situation arises in diffused planar junctions containing a large impurity atom gradient. For illustrative purposes, the magnitude of this gradient is established from the calculated avalanche breakdown properties of an equivalent junction of mesa geometry. In an equivalent mesa junction, this impurity atom gradient should be sufficient to have little influence upon the avalanche breakdown voltage; therefore such a device can be approximated by an asymmetrical abrupt *p-n* junction. Planar junctions containing a large impurity atom gradient exhibit the qualitative avalanche breakdown characteristics of an asymmetrical abrupt (cylindrical) junction, of the type illustrated in Fig. 4b (large impurity atom density inside the circular cylinder). Regions of curvature in this planar junction exhibit a lower breakdown voltage

than the region parallel to the semiconductor surface. This situation implies that junctions of planar geometry (containing a large impurity atom gradient) exhibit a substantially lower theoretical avalanche breakdown voltage than equivalent devices of mesa geometry.

Figures 8 and 9 present the calculated avalanche breakdown voltage for a diffused planar p-n junction. In these illustrations r represents the radius of junction curvature near a diffusion mask edge, C_b is the impurity atom concentration density within the bulk semiconductor material, and α_0 is the impurity atom concentration gradient at the metallurgical junction. In practice, the radius of junction curvature is equivalent to the maximum junction penetration depth in a direction perpendicular to the semiconductor surface. For a particular junction, α_0 is readily calculated from diffusion parameters characterizing the junction fabrication process.

During these calculations (Figs. 8 and 9) it was necessary to terminate each contour of constant radius r when the junction space-charge region extended to the semiconductor surface. Junctions designed to operate beyond this point of termination exhibit surface penetration before avalanche breakdown. For practical engineering purposes, Fig. 10 presents calculations pertaining to the minimum radius of junction curvature, r_m , to ensure that avalanche breakdown occurs at a lower voltage than surface penetra-

Figure 10 Minimum radius of curvature in a diffused planar p-n junction (silicon).



tion. This calculation is based upon the same mathematical model used for avalanche breakdown.

These calculations of minimum junction radius (Fig. 10) resulted in an examination of the design parameters for numerous planar p-n junctions. It was observed that practical laboratory techniques have inadvertently eliminated problems of space-charge penetration. A decrease in junction diffusion depth (and hence a decrease in radius of curvature) is usually accomplished at a constant impurity atom surface concentration; thereby an increase is obtained in the concentration gradient \mathfrak{A}_0 . For this reason, very shallow planar junctions contain a large impurity atom gradient, and their space-charge regions exhibit avalanache breakdown before penetration to the semiconductor surface.

It should be noted that Figs. 8 and 9 partially explain a phenomenon observed in the development of diffused planar transistors. For a given transistor, it has been shown that collector junction avalanche breakdown will occur at approximately 3.5 times its open-base breakdown voltage.10 Measurements indicate frequent deviations from this rule-of-thumb. Some planar transistors undergo openbase breakdown at 75% of their measured collector junction avalanche breakdown voltage. The present calculations (Figs. 8 and 9) indicate that different regions of a planar junction surface can display avalanche breakdown at substantially different voltages. For example, the region of a collector junction under the emitter could be designed to undergo avalanche breakdown at 350 volts, while the edges of this same junction will exhibit breakdown at 130 volts. Calculations indicate that this same junction transistor should exhibit open-base breakdown at 90 to 100 volts.

Acknowledgments

The authors wish to thank Dr. J. Riseman for his support of this effort. In addition, they thank Dr. J. Logan and Mr. P. Murley for many valuable discussions.

References

- 1. G. Gibbons and J. Kocsis, IEEE Trans. ED-12, 193 (1965).
- H. L. Armstrong, E. D. Metz, and I. Weiman, IRE Trans. ED-3, 86 (1956).
- 3. H. L. Armstrong, IRE Trans. ED-4, 15 (1957).
- 4. J. Maserjian, J. Appl. Phys. 30, 1613 (1959).
- D. P. Kennedy and R. R. O'Brien, IRE Trans. ED-9, 478 (1962).
- D. P. Kennedy and R. R. O'Brien, IBM Journal 9, 422 (1965).
- 7. R. M. Scarlett, IRE Trans. ED-6, 405 (1959).
- D. P. Kennedy and R. R. O'Brien, IBM Journal 9, 179 (1965).
- 9. W. Shockley, Bell Syst. Tech. J. 28, 435 (1949).
- D. P. Kennedy and R. R. O'Brien, Int. J. of Elect. 18, 133 (1965).

Received September 27, 1965.